Stability of two-dimensional BN-Si structures

Ernesto D. Sandoval, Samad Hajinazar, and Aleksey N. Kolmogorov

Phys. Rev. B **94**, 094105 — Published 9 September 2016

DOI: 10.1103/PhysRevB.94.094105

Stability of two-dimensional BN-Si structures

E. Sandoval, S. Hajinazar, A.N. Kolmogorov[1]

[1]*Department of Physics, Applied Physics and Astronomy, Binghamton University, State University of New York, PO Box 6000, Binghamton, New York 13902-6000, USA*

Two-dimensional (2D) $BNSi_2$ has been recently proposed to be a viable candidate material with a graphene-like structure. We have carried out *ab initio* evolutionary ground state searches and uncovered a number of 2D structures in the $(BN)_xSi_{1-x}$ pseudobinary system with considerably lower energies. Nevertheless, our formation energy analysis shows that none of these or previously proposed polymorphs are stable with respect to phase separation into 2D Si and BN. Examination of the related CSi, BNC_2, and $BNSi_2$ 2D compounds indicates that the lack of miscibility in the last two systems is due to limited involvement of nitrogen electronic states in the covalent bonding.

The growing interest in 2D materials is fueled by observations and predictions of exotic properties in systems with reduced dimensionality. Graphene displays an array of exceptional mechanical and electronic features, from record tensile strength to supreme electron mobility[1–4]. Downsized to a monolayer, MoS_2 develops a direct and wide bandgap suitable for optoelectronic devices[5]. Recently synthesized silicene, germanene, and stanene are being actively studied for manifestations of quantum Hall effect and topologically nontrivial electronic features[6–8]. 2D boron has been predicted to have a markedly different structural motif[9], now confirmed[10], and to exhibit low-temperature superconductivity[11].

An attractive route to finding new synthesizable materials is consideration of multicomponent systems which leads to a combinatorial explosion of possible configurations. One promising strategy involves identification of bulk compounds with layered morphologies suitable for exfoliation into 2D structures. Examples of such predictive work include high-throughput screening of large experimental databases and rational design of new bulk materials with desired frameworks[12,13]. An alternative strategy involves a direct search for sufficiently stable 2D structures for synthesis with deposition techniques. Evolutionary structure searches, in particular, have been used to identify low-energy structures in C-Si, Sn-S and InP systems[14].

Elemental Si and binary BN systems, being isoelectronic to C, are known to form buckled and flat hexagonal sheets, respectively. The $(BN)_xSi_{1-x}$ pseudobinary system also satisfies the 8-electron rule and could potentially have stable composite 2D structures with desired band gaps. Andriotis *et al.*[15] have considered four hexagonal structures and showed dynamical stability of one-atom-thick $BNSi_2$ configuration. In this study, we have performed an *ab initio* evolutionary search for planar BN-Si compounds and found significantly more stable structures at the $BNSi_2$ composition. However, our assessment of candidate materials' formation energies illustrates a clear tendency for the pseudobinary to decompose into the known BN and Si 2D phases. We have constructed phase boundary geometries and estimated the 1D interface energy to be only a factor of two higher than that in BNC_2. A comparative analysis of the density of states (DOS) in BN, Si, C, $BNSi_2$, CSi, and BNC_2 2D phases provides an explanation for the lack of stability of both $BNSi_2$ and BNC_2 ordered 2D materials.

The problem of global structure optimization can be tackled with various methods based on evolutionary algorithms, particle swarm optimization, minima hopping, random sampling, etc.[16–25] In searches for low-energy 2D structures one needs to introduce a constraint or a selection rule to prevent the structures from becoming 3D[14]. Since BN forms a flat 2D sheet and Si gains only 19 meV/atom from sheet buckling, we adopted a purely flat geometry of the composite structures in our searches. Following examinations of phonon dispersions and nonplanar geometry optimizations showed that some of the considered $BNSi_2$ structures have a tendency to buckle but the distortions lead to insignificant energy gains.

Density functional theory (DFT) calculations have been performed with VASP[26] unless specified otherwise. We employed projector augmented wave potentials[27] and Perdew-Burke-Ernzerhof (PBE) exchange-correlation (xc) functional[28] in the generalized gradient approximation (GGA)[29]. A 500 eV energy cutoff and dense Monkhorst-Pack[30] k-meshes ensured tight numerical convergence. The evolutionary structure optimizations were performed with MAISE package[31] as detailed below. The dynamical stability of select structures was examined with QUANTUM ESPRESSO[32] and PHON[33]. Structure parameters are given in the Supplementary Material[34].

Figure 1 shows competing structures considered in this study at the $BNSi_2$ composition with different number of formula units (n) per cell. All atoms in the previously proposed structure, denoted as (i), have three-fold coordinations but the hexagonal symmetry is broken due to the particular decoration of the lattice with three different species. The centered lattice can be represented with a rectangular conventional cell twice the size of the primitive one. The particular geometry was explained to be favorable as it allows for coexistence of 2.24-Å Si-Si and 1.47-Å B-N bonds close to their near-natural lengths in 2D structures.

A quick visual examination of the structure suggests a simple way of lowering the total energy. The electro-

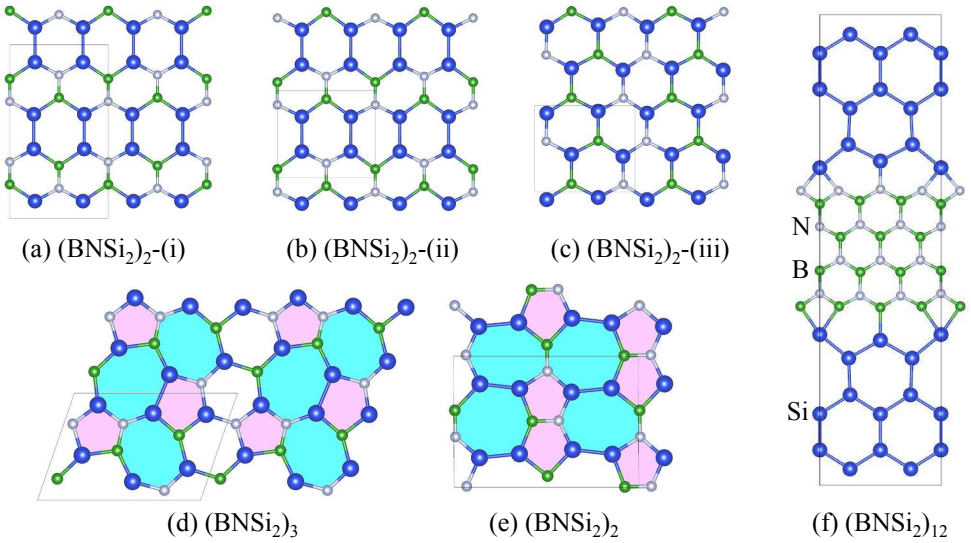

FIG. 1: (color online) Competing planar structures with Si, B, and N shown as blue, green, and grey spheres, respectively. (a) proposed in Ref. 15; (b) constructed by swapping B and N in the bottom rows; (c-e) identified in evolutionary searches; (f) constructed as a phase boundary between Si and BN hexagonal frameworks.

static interaction between B and N atoms would likely get stronger if the B and N atoms in the lowest two rows in Fig. 1(a) were swapped. The adjusted configuration shown in Fig. 1(b) seems more favorable because, while the B-N bonds remain unchanged, the first neighbors across the Si-Si strip are now B-N and N-B instead of B-B and N-N. Our DFT calculations indeed show a higher stability of structure (ii) by 42 meV/atom.

A more systematic search for low-energy structures was performed with an evolutionary search for $(BNSi_2)_n$, $n = 1-4$. The algorithm evolved 16 members in the populations over 50-200 generations depending on the system size. Three runs initiated with different random structures were carried out to illustrate convergence to the same most stable configuration for a given size[16–18]. Fig. 2 shows a typical energy profile for a population in which 70% of children were created via the crossover operation and 30% via mutation. As described in our previous studies[35,36], the former involves merging approximately halves of two random parents and the latter consists of (i) displacing atoms randomly with the Gaussian distribution of width $\sigma_{atom} = 0.2$ Å; (ii) distorting the lattice vectors using a symmetric matrix[37] with random strain components of Gaussian width $\sigma_{lat} = 0.2$; and (iii) swapping atoms with a 30% probability in a random parent. The c axis was kept at 10 Å and the relaxations of in-plane lattice constant and atomic positions were done via conjugate gradient within VASP.

Evolutionary optimizations of $n = 1$ and $n = 2$ unit cells revealed a common motif substantially more stable than the previously proposed one for $BNSi_2$. Fig. 1(c) shows the preference for Si atoms not to form direct bonds with each other which has been seen previously in the related CSi binary (structure (vi) in Ref. 14). There are several ways the non-Si sites can be decorated with B and N. The best $n = 1$ CSi-type structure (not shown) is already 2 meV/atom below (i) while the best $n = 2$ one in Fig. 1(c) is 71 meV/atom below (i).

The key challenge of identifying lowest-energy periodic configurations, as demonstrated in previous studies[36], is that they can occur at arbitrarily large n. Our search for $n = 3$ reveals an even more stable structure, Fig. 1(d), which could have unlikely been constructed manually. The exotic motif still has three-fold coordinated atoms but they are now connected into a network of pentagons, hexagons, and heptagons. According to Euler's

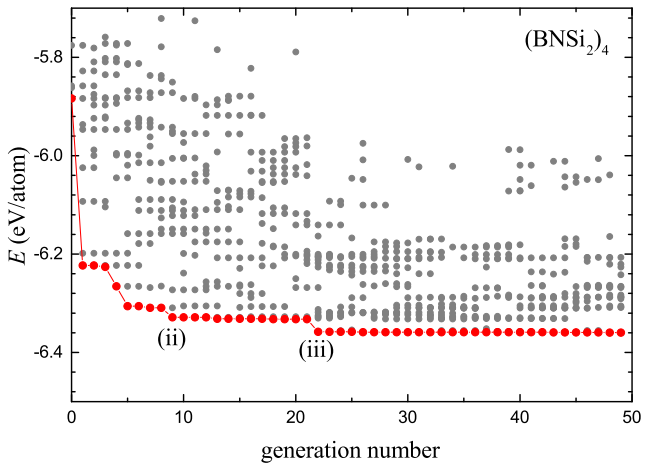

FIG. 2: (color online) Distribution of energies during an evolutionary optimization of 8-atom unit cells at the $BNSi_2$ composition. Candidate structures marked with (ii) and (iii) are shown in Fig. 1.

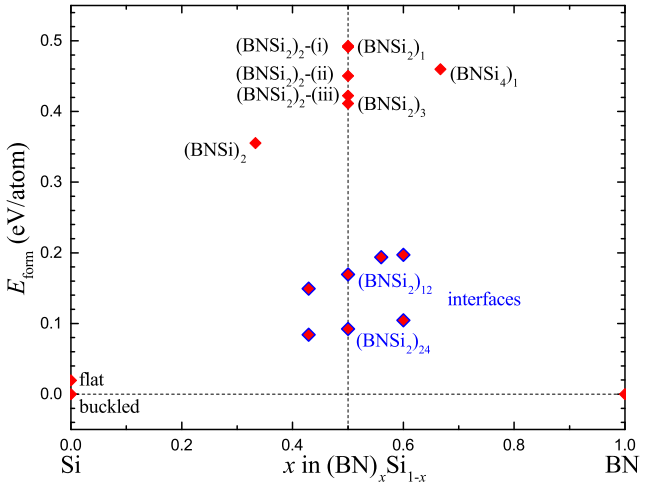

FIG. 3: (color online) Formation energies of planar BN-Si pseudobinary phases with respect to flat hexagonal BN and buckled hexagonal Si structures. The top group of points correspond to considered structures with small $(BNSi_2)_n$ unit cells (up to $n = 3$). The bottom group of points show the energies of interface configurations comprising strips of Si and BN hexagonal networks.

theorem, the matching number of 5- and 7-member rings ensures the same genus of the framework, as discussed in Ref. 38. The network rearrangement lowers the energy further by 11 meV/atom with respect to that of (iii). Interestingly, optimizations of $n = 2, 4$ unit cells produced metastable networks comprised entirely of the 5-7 polygons (Fig. 1(e)) and the most favorable distribution of species corresponded to 31 meV/atom above (i).

Identification of more stable structures is encouraging but does not answer the question regarding their synthesizability until their formation energies are examined. The cohesive energy, defined with respect to *atomic* energies, gives little information about structure's thermodynamic stability. For 3D crystals, for example, negative formation energy with respect to *elemental ground state* energies is a necessary starting check-point but construction of the convex hull across the full composition range is required[39]. For 2D systems the analysis is complicated by the fact that the elemental 2D phases are already only metastable relative to the bulk ground states[14] and can only be produced via specific kinetics-driven routes. In the Si and BN systems of interest, the naturally occurring hexagonal α-BN material is held together by a weak 0.03-eV/atom interlayer bonding[40] but the Si diamond 3D phase is 0.64 eV/atom below its 2D layered counterpart.

Formation energy plot in Fig. 3 demonstrates that none of the discussed structures are expected to form, as they are thermodynamically unstable by over 0.4 eV/atom with respect to not only 3D but also to 2D phases. Since no energetically favorable short-ranged ordering is observed in the rather small unit cells, stable long-ranged ordering is unlikely to occur in larger cells. In other words, one can expect to see lowering of energy via a phase separation into elemental most stable 2D structures.

We constructed a possible grain boundary by taking advantage of the nearly 3:2 ratio between the equilibrium Si-Si (2.25 Å)[41] and B-N (1.45 Å)[42] bond lengths. One can then maintain a three-fold coordination for half of the B-Si and N-Si bonds. Even though the other half are forced to be in a fairly awkward planar four-fold coordinated environment, the overall energy is indeed considerably lower than that of any small-sized configurations with mixed interspecies bonds.

The energy penalty scales only with the length of the interface which explains why the energy per atom in Fig. 3 drops when the size of the Si and BN domains is extended in the transverse direction. We obtained a consistent value[43] of 0.51 ± 0.01 eV/Å for a set of $((BN)_l Si_m)_n$ structures with l:m ratios of (BN):Si and n formula units: $(3{:}4)_4$, $(1{:}2)_{12}$, $(3{:}4)_8$, $(1{:}2)_{24}$, and $(3{:}8)_4$. For comparison, the Si-C interface modeled with the same site arrangements was found to have a 0.54 ± 0.01 eV/Å formation energy. Considering the size similarity of the B-N and C-C bonds, the close energy penalties are not unexpected. However, the two BN-Si and C-Si systems display different propensity for short-range mixing. While the small-cell $BNSi_2$ structures are highly unstable, the hexagonal 2-atom CSi structure has a negative formation energy with respect to the C and Si 2D ground states[14] (-36 meV/atom in our calculations) which is consistent with the observation of CSi flakes in a recent experiment[44].

The density of states (DOS) results presented in Fig. 4 elucidate the underlying reasons for the calculated relative stabilities. A commonly observed structure stabilization feature is the placement of the Fermi level near the bottom of a DOS minimum or, better yet, the full separation of the filled bonding and empty antibonding states. Comparison of the DOS for structures (i) and (ii) in Fig. 4 shows that the B and N swap leads to an overall small upshift of all states but pushes the bonding p_z states near the Fermi level further down deepening the DOS valley. The atomic site decoration in structure (iii) with no direct Si-Si bonds opens up a true bandgap, likely underestimated in the PBE treatment.

The s and p_z states of N, shown as short-dot and solid green lines in Fig. 4, deserve a closer look. For the s-N orbitals in 2D BN, the large overlap with the s orbitals on the 6 N second neighbors along with the small overlap with the s and p_{xy} orbitals on the 3 B nearest neighbors cause a 3.6 eV dispersion. The deep s-N orbitals below -17 eV in the $BNSi_2$ structures (Fig. 4(b-d)) show little overlap with any orbitals other than s-N and, consequently, this band's width depends directly on the number of N-N neighbors. In structures (i-iii), the closest N neighbors are: 2+1 in the third shell, 2 in the third shell, and 2 in the second shell, respectively. The dispersions scale accordingly as 0.6, 0.5, and 1.1 eV. The p_z-N

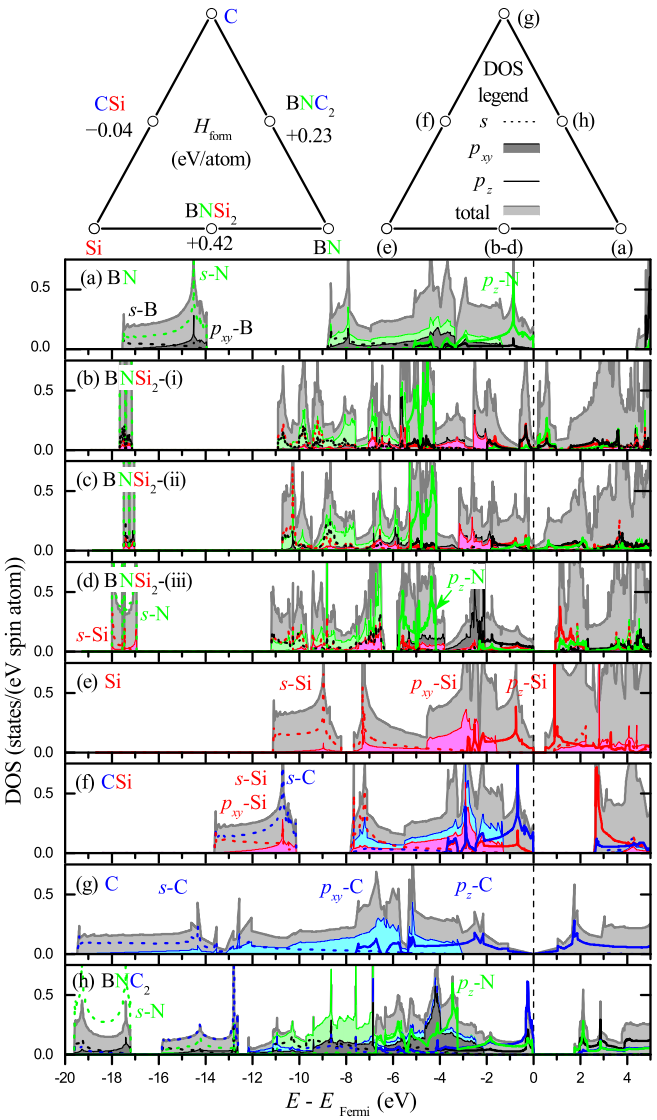

FIG. 4: (color online) The top left diagram shows considered compositions with the corresponding calculated formation energies in the BN-Si-C system. The top right diagram explains the order of the following DOS plots and the legend used to denote DOS characters. Namely, for each Si (red), B (black), N (green), and C (blue) atom, DOS projections on s, p_{xy}, and p_z orbitals are shown as dotted, shaded, and solid lines, respectively. DOS characters for select peaks are labeled explicitly. As discussed in the text, a comparison analysis of the presented 2D materials reveals the width of the s- and p_z-N states to be a key compound stability-defining feature. All DOS values are given per atom to show the total and the partial DOS profiles on the same scale.

bands around -5 eV have a similarly small width, below 2 eV in all (i-iii) structures. Since the bonding and antibonding states for both s- and p_z-N orbitals in $BNSi_2$ are fully filled, their contribution to the total binding is insignificant.

In contrast, the CSi DOS in panel (f) shows a high degree of mixing for C and Si orbitals across the full energy range: s-C and s-p_{xy}-Si between -13.6 and -10.1 eV, s-p_{xy}-C and s-p_{xy}-Si between -7.8 and -1.3 eV, and p_z-C and p_z-Si between -3 and 0 eV. As a result of the strong overlaps the material boasts a 2.6-eV bandgap. Based on these considerations, all valence electrons in CSi contribute to the chemical bonding while half of the N valence electrons in $BNSi_2$-(iii) occupy the more or less localized s and p_z states and do not partake in structure stabilization. It should be noted that the band energy is one of several terms in the DFT total energy but this comparison analysis provides a qualitative explanation for the markedly different calculated formation energies for CSi and $BNSi_2$.

The identified stability factor can be tested on a related BN-C system that has been a subject of numerous studies[45–51]. The poor miscibility of BN and C in 2D has been established both experimentally[47,48] and computationally[49,50]. We examined the most stable structure at the BNC_2 composition reported in Refs. 45,46. The DOS plotted in Fig. 4(h) illsutrates that BNC_2 is part-way between CSi and $BNSi_2$ in terms of the contribution of N electronic states to the covalent bonding: the p_z states are well dispersed as in the former while the s states show insignificant mixing as in the latter. One can then anticipate the formation energy for BNC_2 to be positive and near the average of those for CSi and $BNSi_2$. Our calculated results proved to be in good agreement with this expectation, as 0.23 eV/atom is mid-way between −0.04 eV/atom and 0.42 eV/atom (see top diagram in Fig. 4).

For evaluation of interface energetics in BNC_2, we used previously considered armchair, zigzag-A, and zigzag-B geometries[51] on a shared hexagonal network and found the respective interface energies to be 0.23, 0.30, and 0.71 eV/Å. The findings are in good agreement with previously calculated results[51] as well as with experimental observations of phase boundaries, predominantly of the armchair and zigzag-A type, in synthesized BN-C 2D hexagonal frameworks[47]. Notably, the energy of the interface with mismatched lattices in $BNSi_2$ is only about a factor of two higher than the lowest one in BNC_2. It would be interesting to check experimentally if BN and Si monoloayers could fuse and form such phase boundaries.

A structure represents at least a local minimum at $T = 0$ K if all of the phonon mode frequencies have real values. Conclusive demonstration of structure's dynamical stability can be a demanding task because accurate evaluation of phonon softening requires a proper choice of approximations and convergence settings. For example, the HSE hybrid functional employed in the previous study of $BNSi_2$ has been recently shown to have problems assessing lattice stability in metallic systems[52]. We calculated phonon dispersions for the (i-iii) structures using PAW-PBE scalar relativistic pseudopotentials (pbe.0.3.1)[53] and the linear response method as implemented in QUANTUM ESPRESSO. Dense k-meshes ensured good convergence of the phonon frequencies at

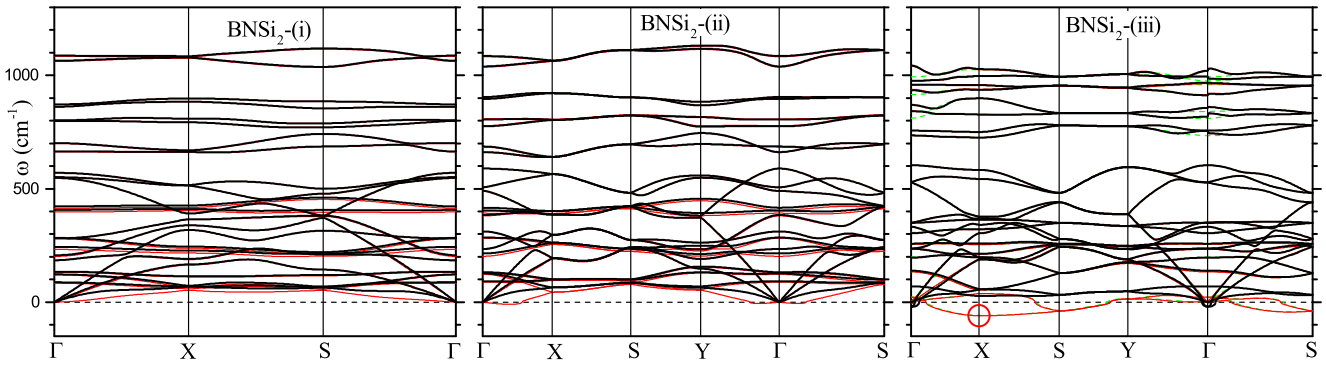

FIG. 5: Phonon dispersions calculated with the linear response method for three $BNSi_2$ structures. The black thick (thin red) lines denote results obtained with the 'crystal' ('simple') acoustic sum rule as defined in QUANTUM ESPRESSO[32]. For the semiconducting structure (iii), the dashed green lines denote the results obtained with the 'simple' acoustic sum rule but without the polar corrections and show 20-50 cm−1 splitting for a few high-frequency optical modes near Γ.

each q point and the phonon dispersions were found to be well converged with respect to the size of the q-meshes[54]. However, Fig. 5 shows two very different dispersion sets depending on which acoustic summation rule, 'simple' or 'crystal'[32,55], was applied. In this postprocessing step the interatomic force constants are adjusted to prevent the acoustic mode frequencies from deviating from zero at the Γ point; the latter implementation, additionally, minimizes the deviations in the interatomic force constants with respect to the original *ab initio* set. Note that the polar correction for the semiconducting structure (iii) causes a 20-50 cm^{-1} LO-TO split for the highest optical modes (Fig. 5(c)) and a small kink for an acoustic mode near the Γ point (Fig. 6(a)) after the application of the acoustic sum rule. We repeated the calculations with the frozen phonon method as implemented in PHON coupled with VASP. For structure (i), the lowest branch along Γ-X ended up in the imaginary region with a small $\sim 8i$-cm^{-1} value around the (1/6,0,0) q-point[56]. For structure (iii), the X-point frequency of the softest mode was consistent with the $60i$-cm^{-1} value obtained in the linear response calculations.

In order to determine whether these flat configurations indeed have a propensity toward buckling and to estimate possible values of distortion-induced stabilization we have examined structure (iii) in more detail. Following the eigenvector corresponding to the optical mode with the imaginary frequency of $60i$ cm^{-1} at the X-point, we obtained a slightly buckled phase[34], with maximum 0.4 Å out-of-plane deviations, 2.1 meV/atom below that of the parent structure (see Fig. 6(b))[57]. Follow-up phonon calculations revealed the presence of additional imaginary modes remaining in the obtained structure which would need to be dealt with by systematically increasing the unit cell size[36,58]. The large number and size of possible derived structures quickly makes the procedure prohibitively expensive. Considering that the (i-iii) structures have positive formation energies exceeding 0.4 eV/atom, identification of any viable metastable derivatives in this way is highly unlikely. Molecular dynamics (MD) with material-dependent simulation settings can be helpful for locating structures' nearby local minima. For the covalently bonded BNS_2, 12-ps MD runs at 1000 K in Ref. 15 did not identify the related honeycomb configurations with swapped atoms shown in this study to have lower energy. MD-based identification of (meta)stable polymorphs derived from dynamically unstable parent structures is rather difficult, as it involves considering

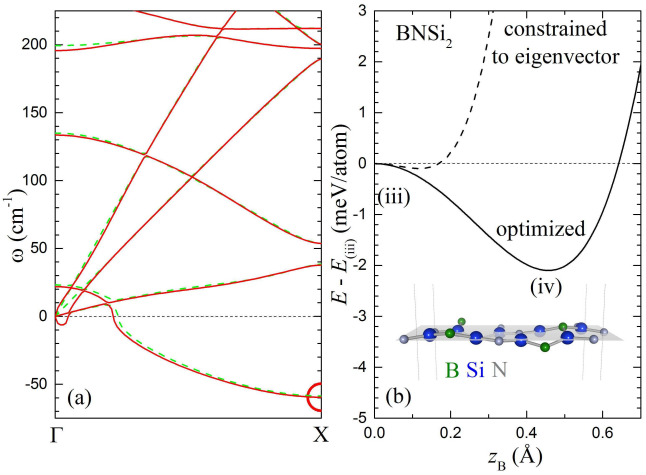

FIG. 6: (color online) (a) Low-frequency modes for $BNSi_2$-(iii) calculated with linear response and postprocessed with the 'simple' acoustic sum rule. The dashed green lines correspond to the results obtained without the polar corrections and indicate insignificant changes in the low-frequency modes. (b) Energy profiles as a function of the z coordinate of B atom for the $2 \times 1 \times 1$ supercell modulated along the eigenvector corresponding to the imaginary frequency at $q = (0.5, 0, 0)$. The solid line data was calculated with all in-plane structural parameters fully relaxed and the minimum corresponds to the buckled structure (iv).

specific supercells and performing careful annealing.

Use of substrates can preferentially stabilize a particular phase with a matched lattice[59]. The interaction of 2D BN with most metallic substrates is fairly weak[60]; for Ag(111) it is -0.066 meV/atom in the vdW-DF treatment[61]. The interaction between 2D Si and metallic substrates is of covalent nature and considerably stronger; for Ag(111) it is -0.652 eV/atom in vdW-DF[62]. As a crude estimate, we calculated binding energy for BNSi2-(i) on Ag(111) which have a lattice mismatch of 8%. Even without considering the stain-induced penalty, the lowest -0.40 eV/atom obtained with vdW-DF for BNSi2-(i) turned out to be only -0.04 eV/atom below the -0.36 eV/atom average binding in the BN/Ag(111) and Si/Ag(111) systems. Finding a matching lattice for the more stable but more complex 5-6-7 $BNSi_2$ network is far more challenging. Even if suitable substrates are found the relative gain in binding energy is not expected to make up for the large positive 0.42-0.49 eV/atom values of the $BNSi_2$ formation energy.

In conclusion, we have demonstrated the presence of more energetically favorable 2D configurations compared to previously proposed ones for the $BNSi_2$ compound. Simple rearrangements of atoms on the hexagonal lattice lead to a more favorable DOS and turn the metal into a semiconductor. Even more stable exotic networks with 5-6-7 polygons were identified with an *ab initio* evolutionary search. However, all the structures have been shown to have relatively high formation energies with respect to elemental 2D Si and BN polymorphs and are not expected to form. A comparative analysis of DOS profiles in related CSi, BNC_2, and $BNSi_2$ phases revealed that not all valence electrons in the last two are fully engaged in the covalent bonding. The findings are consistent with the lack of observed ordered BNC_2 or $BNSi_2$ 2D materials. Future efforts to design stable 2D configurations at other compositions, e.g., in the expanded BN-C-Si system, should take into consideration non-hexagonal morphologies and carefully manage the size and the electronic state energy characteristics of the constituent elements.

The authors gratefully acknowledge the NSF support (Award No. DMR-1410514) and helpful discussions with Roxana Margine and Feliciano Giustino.

[1] K. S. Novoselov, A. K. Geim, S. V. Morozov, D. Jiang, Y. Zhang, S. V. Dubonos, I. V. Grigorieva, and A. A. Firsov, Science **306**, 666 (2004).

[2] K. I. Bolotin, K. J. Sikes, Z. Jiang, M. Klima, G. Fundenberg, J. Hone, P. Kim, and H. L. Stormer, Solid State Commun. **146**, 351 (2008).

[3] C. Lee, X. Wei, J. W. Kysar, and J. Hone, Science **321**, 385 (2008).

[4] J. Moser, A. Barreiro, and A. Bachtold, Appl. Phys. Lett. **91**, 163513 (2007).

[5] K. F. Mak, C. Lee, J. Hone, J. Shan, and T. F. Heinz, Phys. Rev. Lett. **105**, 136805 (2010).

[6] M. Houssa, G. Pourtois, V. V. Afanas'ev, and A. Stesmans, Appl. Phys. Lett. **96**, 082111 (2010).

[7] S. Lebegue and O. Eriksson, Phys. Rev. B **79**, 115409 (2009).

[8] S. Balendhran, S. Walia, H. Nili, S. Sriram, and M. Bhaskaran, Small **6**, 640 (2015).

[9] X. Wu, J. Dai, Y. Zhao, Z. Zhuo, J. Yang, and X. C. Zeng, ACS Nano, **6** (8), 7443 (2012)

[10] B. Feng, J. Zhang, Q. Zhong, W. Li, S. Li, H. Li, P. Cheng, S. Meng, L. Chen, and K. Wu, Nat. Chem. (to be published), (2016).

[11] Y. Zhao, S. Zeng, and J. Ni, Phys. Rev. B **93**, 014502 (2016).

[12] S. Lebegue, T. Bjorkman, M. Klintenberg, R. M. Nieminen, and O. Eriksson, Phys. Rev. X **3**, 031002 (2013).

[13] J. Shao, C. Beaufils, and A.N. Kolmogorov, Scientific Reports, (to be published) (2016).

[14] B. C. Revard, W. W. Tipton, A. Yesypenko, and R. G. Hennig, Phys. Rev. B **93**, 054117 (2016).

[15] A. N. Andriotis, E. Richter, and M. Menon, Phys. Rev. B **93**, 081413 (2016).

[16] T.S. Bush, C. R. A. Catlow, and P. D. Battle, J. Mater. Chem. **5**, 1269 (1995)

[17] N. L. Abraham and M.I.J. Probert, Phys. Rev. B **73**, 224104 (2006).

[18] A. R. Oganov and C. W. Glass, J. Chem. Phys. **124**, 244704 (2016).

[19] G. Trimarchi and A. Zunger, Phys. Rev. B **75**, 104113 (2007).

[20] D. J. Wales and J. P. K. Doye, J. Phys. Chem. A **101**, 5111 (1997).

[21] D. J. Wales and H. A. Scheraga, Science **285**, 1368 (1999).

[22] M. Amsler and S. Goedecker, J. Chem. Phys. **133**, 224104 (2010).

[23] C. J. Pickard and R. J. Needs, Phys. Rev. Lett. **97**, 045504 (2006).

[24] Y. Wang, J. Lv, L. Zhu, and Y. Ma, Phys. Rev. B **82**, 094116 (2010).

[25] Y. Wang, J. Lv, L. Zhu, Y. Ma, Comput. Phys. Commun. **183**, 2063 (2012).

[26] G. Kresse and J. Hafner, Phys. Rev. B **47**, 558 (1993); G. Kresse and J. Furthmüller, Phys. Rev. B **54**, 11169 (1996).

[27] P.E. Blöchl, Phys. Rev. B **50**, 17953 (1994).

[28] J. P. Perdew, K. Burke, and M. Ernzerhof, Phys. Rev. Lett. **77**, 3865 (1996).

[29] J.P. Perdew, K. Burke, and M. Ernzerhof, Phys. Rev. Lett. **78**, 1396 (1997).

[30] J. D. Pack and H. J. Monkhorst, Phys. Rev. B **13**, 5188 (1976); **16**, 1748 (1977).

[31] A. N. Kolmogorov, http:\\maise-guide.org

[32] P. Giannozzi *et al.*, J. Phys.: Condens. Matter, **21**, 395502 (2009).

[33] D. Alfè, Comp. Phys. Commun. **180**, 2622 (2009).

[34] See EPAPS Document No. 1.

[35] A. N. Kolmogorov, S. Shah, E. R. Margine, A. F. Bialon, T. Hammerschmidt, and R. Drautz, Phys. Rev. Lett. **105**, 217003 (2010).

[36] A. N. Kolmogorov, S. Shah, E. R. Margine, A. K. Kleppe,

and A. P. Jephcoat, Phys. Rev. Lett. **109**, 075501 (2012).
[37] A.R. Oganov and C.W.J. Glass, Chem. Phys. **124**, 244704 (2006)
[38] E. R. Margine, A. N. Kolmogorov, D. Stojkovic, J. O. Sofo, and V. H. Crespi, Phys. Rev. B **76**, 115436 (2007).
[39] A. G. Van Der Geest and A. N. Kolmogorov, CALPHAD **46**, 184 (2014).
[40] H. Rydberg, M. Dion, N. Jacobson, E. Schrøder, P. Hyldgaard, S. I. Simak, D. C. Langreth, and B. I. Lundqvist, Phys. Rev. **91**, 126402 (2003).
[41] P. D Padova, C. Quaresima, C. Ottaviani, P. M. Sheverdyaeva, P. Moras, C. Carbone, D. Topwal, B. Olivieri, A. Kara, H.Oughaddou, B. Aufray, and G. Le Lay, App. Phys. Lett. **96**, 261905 (2010).
[42] Y. Stehle, H. M. Meyer, R. R. Unocic, M. Kidder, G. Polizos, P. G. Datskos, R. Jackson, S. N. Smirnov, and I. V. Vlassiouk, Chem. Mat. **27**, 8041 (2015).
[43] We give the average value for the two non-equivalent interfaces in the simulation cell (Fig. 1(f)). In all BN-Si and C-Si interface simulations the in-plane lattice constants were relaxed along with the atomic positions.
[44] S. S. Lin, J.Phys. Chem. C **116**(6), 3951 (2012).
[45] A. Y. Liu, R. M. Wentzcovitch, and M. L. Cohen, Phys. Rev. B **39**, 1760 (1989).
[46] H. Nozaki, S. Itoh, J. Phys. Chem. Solids **57**, 41 (1996)
[47] L. Ci *et al*, Nat. Mater. **9**, 430 (2010)
[48] P. Sutter, R. Cortes, J. Lahiri and E. Sutter, Nano Lett. **12** , 4869 (2012)
[49] S. Azevedo, Phys. Lett. A **351**, 109 (2006)
[50] K. Yuge, Phys. Rev. B **79**, 144109 (2009)
[51] R. S. Krsmanovic and Z. Slijvancanin, J. Phys. Chem. C **118**, 16104 (2014)
[52] W. Gao, T. A. Abtew, T. Cai, Y. Sun, S. Zhang, and P. Zhang, Solid State Commun. **234**, 10 (2016).
[53] A. Dal Corso, Comput. Mater. Sci. **95**, 337 (2014).
[54] 0.02 Ry smearing, 45 Ry wavefunctions cutoff, and 270 Ry charge density cutoff were used in the linear response calculations. For all three $BNSi_2$ structures we used the 12×12 k-point meshes in the $x - y$ plane. The q meshes were chosen to be 6×6, 4×4, and 6×6 for structures (i-iii), respectively. For structures (i) and (iii) we checked that the 4×4 q-point mesh produced virtually identical phonon dispersions.
[55] N. Mounet, M.S thesis, Massachusetts Institute of Technology, 2005.
[56] We used a 4×4 k-mesh and a 3×3 expansion of the 8-atom primitive cell for $BNSi_2$(ii), a 6×6 k-mesh in a 2×2 supercell for $BNSi_2$-(ii), and a 4×4 k-mesh in a 3×3 supercell for $BNSi_2$-(iii). For structure (i), we tried different displacement values (0.040 Å, 0.025 Å, 0.02 Å, 0.01 Å), a denser k-mesh (6×6), and a larger c axis (20Å) but observed close $8i$ cm^{-1} values for the imaginary mode at $q = (1/6, 0, 0)$ with all these settings. Varying the displacement values had little effect on the dispersion for structure (iii) as well.
[57] QUANTUM ESPRESSO calculations produced close values for structures (i-iii) relative to the identified buckled derivative: 72.4, 28.9 and 3.1 meV/atom compared to 72.9, 30.5, and 2.1 meV/atom in VASP.
[58] A. Togo and I. Tanaka, Phys. Rev. B **87**, 184104 (2013).
[59] V. Ozolins, C. Wolverton, A. Zunger, Phys. Rev. B **57**, 4816 (1998).
[60] M. Bokdam, G. Brocks, M. I. Katsnelson, and P. J. Kelly, Phys. Rev. B **90**, 085415 (2014).
[61] J. Klime, D. R. Bowler, and A. Michaelides, J. Phys. Cond. Matt. **22**, 022201 (2010).
[62] Z. X. Guo, S. Furuya, J. I. Iwata, and A. Oshiyama, Phys. Rev. B **87**, 235435 (2013).